

# Land cover, surface temperature and leaf area index maps from satellites used for the aggregation of momentum and temperature roughnesses

Charlotte B. Hasager\*, Niels Otto Jensen\*, Albert Olioso<sup>+</sup>

\*Risø National Laboratory, Wind Energy Department, Roskilde, Denmark

<sup>+</sup>INRA Bioclimatologie, Domaine Saint-Paul, Avignon, France

[charlotte.hasager@risoe.dk](mailto:charlotte.hasager@risoe.dk), [n.o.jensen@risoe.dk](mailto:n.o.jensen@risoe.dk), [olioso@avignon.inra.fr](mailto:olioso@avignon.inra.fr)

**ABSTRACT-** *A new concept for aggregation (area-averaging) of the roughness lengths for the momentum and sensible heat flux is described. The result are the so-called effective roughness values that are useful for the calculation of the surface energy balance and surface fluxes at larger scales e.g. in climate models, weather forecasts and hydrological modelling in heterogeneous landscapes. Typically a ratio between the momentum roughness,  $z_{0m}$ , and temperature roughness,  $z_{0t}$ , of the order of 1 or 10 is assumed. In the current work the roughnesses are directly calculated based on a set of linearized atmospheric flow equations. The equations are solved by Fast Fourier Transforms and iteratively solved in regard to stability (Monin-Obukhov similarity scaling), viscous sub-layer resistance and water roughness (Charnock). The microscale model calculates the area-average of  $\langle z_{0m} \rangle$  and  $\langle z_{0t} \rangle$  for each large grid cell containing a number of local microscale patches of the size order of 30-1000 m. At this horizontal length scale the non-linear advective effects are highly significant. The results from a case study in the Alpilles area in France are presented. The model inputs are surface temperature maps, leaf area index maps and land cover maps based on high-resolution optical satellite or airborne scenes. The local roughness length for momentum is assigned per pixel based on land cover type and vegetation height. For bare soil, water and urban area there is a constant ratio between the local values of  $z_{0m}$  and  $z_{0t}$  but in vegetated areas the ratio is dependent upon vegetation type and leaf area index. Therefore  $\langle z_{0m} \rangle$  and  $\langle z_{0t} \rangle$  are no longer proportional.*

## 1 INTRODUCTION

There is a need to calculate the aggregated, i.e. non-linearly area-averaged, values of the roughness lengths for momentum and scalars because these effective values are necessary input to many regional and global scale atmospheric models used for weather prediction, climate simulations as well as in hydrological applications. Microscale heterogeneities, i.e. surface changes in the spatial domain of the order of 100 m to 1000 m, are very important for the total grid averaged surface stress and the grid averaged surface heat fluxes. The need to find practical and fast aggregation routines for the roughnesses is a well-known problem (e.g. Viterbo 1996, Sellers et al. 1996). Area-averaging the roughness by simple area-weighted averaging is not physically sound. This is due to the highly non-linear turbulent responses of the atmospheric flow.

Recently an objective, physically-based model that takes the turbulent response of the atmospheric flow into account for every roughness step change in the terrain was developed. The solution is numerical fast because the linearized flow equations are solved by

Fast Fourier Transforms (Hasager and Jensen, 1999). The model is a so-called microscale surface-flux aggregation model in 2-dimensions in the horizontal domain.

Briefly described the microscale aggregation model needs input of high-resolution maps of roughness, land cover type, leaf area index (LAI) and surface temperature and a known wind speed, wind direction and air temperature at the computational level (e.g. the lowest level of the Météo France Arpège model at 25m). The flow equations include correction for atmospheric stability (Monin-Obukhov similarity scaling). This is iteratively calculated in every pixel. The friction velocity and sensible heat flux is calculated pixel-wise in the domain and area-averaged non-linearly to the desired grid cell size of low-resolution satellite data such as NOAA AVHRR 1 km grid cells (Wassenaar et al. 2002) or mesoscale climate models (Hasager et al. 2002a).

The model outputs are 1) the effective roughness length for momentum,  $\langle z_{0m} \rangle$  that always will be larger than a logarithmic average due to the *added* effect of non-equilibrium flow conditions, 2) the effective

scalar roughness length,  $\langle z_{0t} \rangle$  (for heat, water vapour and passive scalars) that generally will be smaller than for equilibrium conditions (Wood and Mason, 1991), 3) the friction velocity map, 4) the scalar scale map and 5) the sensible heat flux map. The maps have the same spatial resolution as the input maps.

It is seen as an advantage to calculate  $\langle z_{0t} \rangle$  directly instead of estimating it as a fraction of  $\langle z_0 \rangle$  for surface-flux calculation.

The logarithmic ratio between the two roughness values is named the  $kB^{-1}$  value. For homogeneous surfaces with porous vegetation a value of 2.3 is often assumed valid (see Hasager, 1997), but worldwide experimental evidence shows a very large variation (e.g. Mölders et al., 1998).

The overall goal of calculating the effective roughness for scalar transport is to achieve very precise area-averages of the surface fluxes. For very large patches equilibrium conditions will apply, but for shorter horizontal length scales typical for instance in the Alpilles area in France, non-equilibrium conditions is expected to dominate the scalar surface fluxes.

## 2 THEORETICAL PART

In surface-layer profile relations it has been customary to take the roughness length for temperature  $z_{0t}$  equal to  $z_0$  for momentum. However, especially if  $z_0$  includes the effect of separated flow over orography this can lead to quite erroneous results for the heat flux. In the following we will assume that  $z_0$  is the micrometeorological roughness, but as we will show below,  $z_{0t}$  is in general less than  $z_0$ . How much smaller depends on the type of the surface, and unfortunately also on the value of the friction velocity  $u_*$ . Recently the formal dependence was presented by Jensen et al. (2002) and is described in detail in the following. Note, we reserve brackets e.g.  $\langle z_0 \rangle$  to signify spatial averages as opposed to  $z_0$  for local values.

Per definition we have

$$u_* r_a = \frac{u}{u_*} = \frac{1}{\kappa} \left( \ln \frac{z}{z_0} - \Psi_M \left( \frac{z}{L} \right) \right) \quad (1)$$

where  $u_*$  is the friction velocity,  $r_a$  is the aerodynamic resistance,  $u$  is the mean wind speed,  $\kappa$  the von Kármán constant ( $\approx 0.4$ ),  $z$  is the height above the displacement distance of the vegetation, and  $z_0$  is the aerodynamic roughness.

The correction function,  $\Psi_M$  which depends on atmospheric stability expressed by the Monin-Obukhov length

$$L = \frac{u_*^2}{\kappa \frac{g}{T} \theta_*} \quad (2)$$

is an empirically determined function (fitted analytical function). While  $r_a$  is the only limiting resistance for “deposition” of momentum, scalars<sup>1</sup> such as temperature and humidity have an additional resistance  $r_b$  because they are also limited by molecular diffusion through the viscous sub-layers that blanket all surfaces. Thus for temperature

$$u_* (r_a + r_b) = \frac{\theta - \theta_0}{\theta_*} = \frac{1}{\kappa} \left( \ln \frac{z}{z_{0t}} - \Psi_H \left( \frac{z}{L} \right) \right) \quad (3)$$

where  $\theta$  is the temperature at height  $z$ ,  $\theta_0$  is the surface temperature and  $\theta_*$  is a scale for the temperature fluctuations ( $\theta_* u_*$  is the sensible heat flux,  $H$ ).  $z_{0t}$  is the roughness for temperature and  $\Psi_H$  is the Monin-Obukhov function for heat flux. Implicitly, eq. (3) assumes that the von Kármán constant as well as the displacement distance are the same for a scalar as for momentum. From eqs.(1) and (2) it follows that

$$u_* r_b = \frac{1}{\kappa} \left[ \ln \frac{z_0}{z_{0t}} - \left( \Psi_H \left( \frac{z}{L} \right) - \Psi_M \left( \frac{z}{L} \right) \right) \right] \quad (4)$$

This equation establishes the intimate connection between  $r_b$  and  $z_{0t}$ . In the following we shall neglect the subtle difference between  $\Psi_H$  and  $\Psi_M$  which then leads to the simple relationship

$$z_{0t} = \frac{z_0}{\exp(\kappa u_* r_b)}. \quad (5)$$

For smooth surfaces  $z_0$  and  $z_{0t}$  in eq.(4) are replaced by the molecular sub-layer thickness  $\nu/u_*$  and  $D/u_*$  respectively, leading to a fixed ratio between the momentum and temperature roughness and

$$z_{0t} = \frac{z_0}{Pr} \quad (6)$$

where  $Pr$  is the Prandtl number ( $\approx 0.7$ ) equal to the kinematic viscosity  $\nu$  ( $\approx 1.5 \cdot 10^{-5} \text{ m}^2 \text{ s}^{-1}$ ) divided by the molecular heat conductivity  $D$  ( $\approx 2 \cdot 10^{-5} \text{ m}^2 \text{ s}^{-1}$ ). In practice this will occur only over water surfaces under low wind conditions (at about  $u_* < 0.1 \text{ m s}^{-1}$  or  $u_{10m}$  less than  $3.3 \text{ m s}^{-1}$ ).

<sup>1</sup> although temperature and humidity have some influence on buoyancy they are for some practical purposes regarded as passive contaminants

The above implies that  $u_* r_b$  is constant for smooth surfaces. However, in general this product is not a constant but is in itself a function of  $u_*$ . Hence it is immediately seen from eq.(5) that  $z_{0t}$  is not a property of the surface alone but depends on the flow.

## 2.1 Expressions for the additional resistance: $r_b$

As mentioned above  $u_* r_b$  is not in general a constant. It is customary to describe its variation in relation to the roughness Reynolds number

$$Re = \frac{z_0 u_*}{\nu} \quad (7)$$

Figure 1, adapted from Garratt and Hicks (1973), shows such dependencies. The striking thing is the difference between rough surfaces consisting of bluff elements and rough surfaces consisting of plants (fibrous canopies).

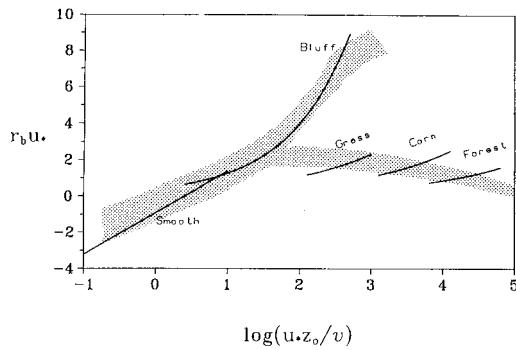


Figure 1 Adapted from Garratt and Hicks (1973). Note that there is an error in the label on the ordinate axis. It should have been  $\kappa r_b u_*$ .

The bluff body branch on the figure can be described by the relation

$$\kappa r_b u_* = c \Pr(Re)^{1/2} \quad (8)$$

The types of land cover categories where this equation applies ranges from water bodies that are aerodynamically rough ( $u_* > 0.1$  m/s) over ice, snow and bare soils to cities. However, it turns out that for large  $z_0$  values, the values of  $z_{0t}$  become unrealistically small (e.g.  $10^{-40}$  m). So it is concluded that the relation in eq. (8) is not realistic for large values of  $Re$ . Therefore a modified expression is sought.

It is suggested to express  $Re$  as a function of the length scale of typical materials over which the development of laminar layers at the urban surfaces takes place, e.g. bricks, roof materials etc. In fact the method is similar in concept to the one applied for plant canopies by Jensen and Hummelshøj (1995). In other words, the laminar layers do not scale with the height of the

buildings but rather with the smaller scale features of the urban surfaces, e.g. roof tiles, windows, etc.

$$Re = \frac{l u_*}{\nu} \quad l = \begin{cases} z_0 & \text{if } z_0 < 0.05 \text{ m} \\ 0.05 & \text{if } z_0 \geq 0.05 \text{ m} \end{cases} \quad (9)$$

Thus by combining eqs. 5 and 9 we get

$$\ln \frac{z_0}{z_{0t}} = c \Pr \left( \frac{l u_*}{\nu} \right)^{1/2} \quad (10)$$

The factor  $c \Pr$  in the above equation is assessed to be about 0.4.

In the MKS unit system we thus have the following practical expressions for non-vegetated land surfaces

$$z_{0t} = \frac{z_0}{\exp(100 \sqrt{z_0 u_*})} \quad \text{for } z_0 < 0.05 \text{ m} \quad (11)$$

and

$$z_{0t} = \frac{z_0}{\exp(22 \sqrt{u_*})} \quad \text{for } z_0 \geq 0.05 \text{ m} \quad (12)$$

Figure 2 shows the variation of  $z_{0t}$  as a function of  $z_0$  for non-vegetated surfaces and it is seen that  $z_{0t}$  varies several orders of magnitude.

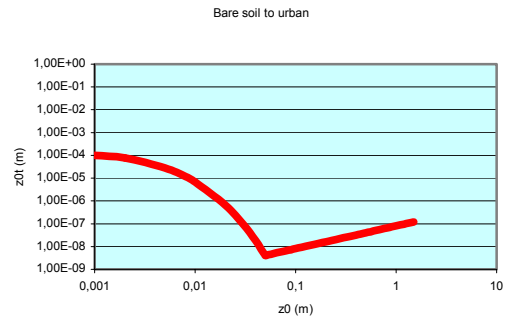


Figure 2  $z_{0t}$  in m as a function of  $z_0$  for non-vegetated surfaces for  $u_* 0.5 \text{ m s}^{-1}$ .

Over water the description is complicated by the fact that the roughness  $z_0$  depends on  $u_*$  through Charnock's formula (Charnock, 1955)

$$z_0 = \alpha \frac{u_*^2}{g} \quad (13)$$

where  $g$  ( $9.81 \text{ m s}^{-2}$ ) is the constant of gravity and  $\alpha \approx 0.015$  but where the exact value actually depends on the wave age, the fetch length and probably also the water depth at least over shallow water.

For smooth water, i.e. for  $u_* < 0.1$

$$z_{0t} = z_0; \quad z_0 = 0.1 \nu / u_* \quad (14)$$

$$\nu \approx 1.5 \cdot 10^{-5} \text{ m}^2 \text{ s}^{-1}.$$

For rough water, i.e. for  $u_* > 0.1$

$$z_{ot} = \frac{z_o}{\exp(100(z_o u_*)^{1/2})}; z_o = 0.015 \frac{u_*^2}{g} \quad (15)$$

The plant canopy branch (see Figure 1) on the other hand has literally no dependence on Re. It was shown by Jensen and Hummelshøj (1995) that this is because the length scale  $z_o$  is not relevant. For example  $z_o$  for a forest is very large but what controls  $r_{bs}$ , or more precisely the thickness of the viscous sub-layers is the dimensions  $l$  of the fibrous elements. For plant canopies Jensen and Hummelshøj (1997) give

$$r_b u_* = c \frac{\text{Pr}}{\text{LAI}^{2/3}} \left( \frac{l u_*}{\nu} \right)^{1/3} \quad (16)$$

where  $\text{LAI}$  is the leaf area index, the Prandtl number has already been defined and  $c$  here is a constant of about 5. The length scale  $l$  is around  $3 \cdot 10^{-3}$  m for grass, grains and conifer forest and around  $3 \cdot 10^{-2}$  m for deciduous forest in leaves.

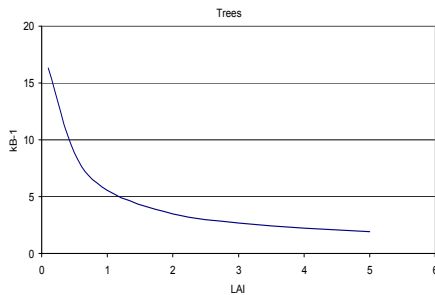
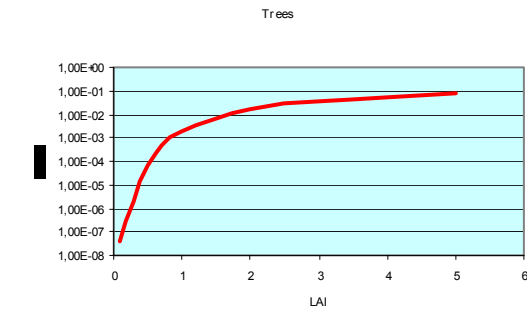


Figure 3 a)  $z_{0t}$  in m as a function of LAI and b)  $kB^{-1}$  as a function of LAI for forest with  $z_0$  0.5 m.

For vegetated land

$$z_{ot} = \frac{z_o}{\exp\left(\frac{5.85}{\text{LAI}^{2/3}} u_*^{1/3}\right)} \quad (17)$$

Figure 3a and b show the variation of  $z_{0t}$  and  $kB^{-1}$  as a function of  $\text{LAI}$  for forest, respectively. The value of

$z_{0t}$  varies several orders of magnitude and for large values of  $\text{LAI}$  the value of  $kB^{-1}$  approaches 2.3.

### 3 THE AGGREGATION PROGRAMME

The new model development is an explicit calculation of the effective roughness for temperature  $\langle z_{0t} \rangle$ . The approach is to apply a set of equations valid for local conditions for the different land cover types in the terrain for  $z_{0t}$  and iteratively solve these.

The model runs on pc and the calculation for a  $512 \cdot 512$  domain (e.g. a 15 km \* 15 km region with an input of 30 m \* 30 m resolution) is achieved typically in less than 10 seconds computational time. Figure 4 shows a schematic of the model components.

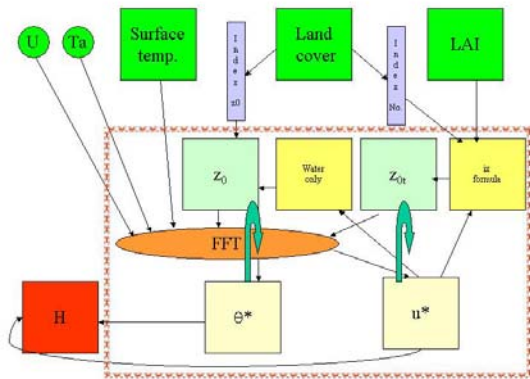


Figure 4 Schematic of the surface-flux microscale aggregation model. The inputs are mean wind speed ( $u$ ) and direction, air temperature ( $T_a$ ) at the computational level and maps of surface temperature, land cover classes and LAI from satellite or airborne Earth observation data. The aerodynamic roughness map ( $z_0$ ) is generated from an index list except for water bodies where the Charnock's relationship is used. The index number and  $z_0$ -equation (ix-formula) are prescribed for each land cover type to provide the initial  $z_{0t}$  map (eqs.11, 12, 14, 15 and 17). The model runs within the dotted line. The linearized atmospheric flow equations are solved by FFT. The output maps are the friction velocity ( $u_*$ ), the temperature scalar ( $\theta_*$ ), the roughness map ( $z_0$ ) and the scalar roughness map ( $z_{0t}$ ) all of which are found through iteration (indicated by the curved arrows). The iteration is due to the stability function (Monin-Obukhov similarity scaling) and the Charnock's relationship. The final outputs are a map of the sensible heat flux ( $H$ ) and the effective roughness for momentum  $\langle z_0 \rangle$  and for scalar transport  $\langle z_{0t} \rangle$  calculated directly.

## 4 ALPILLES CASE STUDY

### 4.1 Experimental site and remote sensing data

The experimental site in the Alpilles area is located in the south of France (N43°47', E4°45') and the measurement campaign was from October 1996 to November 1997. The ground-based study involved surface-flux observations in various crops e.g. wheat, sunflower, maize, alfalfa (Oliosio et al. 2002a). Other dominant land cover types within the 5 km by 5 km study area are orchards and forest.

The airborne observations include PoLDER and thermal scenes (Jacobs et al. 2002). The thermal scanner was flown at 1500 m and 3000 m height on a total of 18 days. The thermal images were calculated into radiant surface temperature maps including correction for emissivity and the roughness maps were produced from combining land cover information and vegetation height from field studies (Oliosio et al. 2002b). The *LAI* maps were retrieved from airborne PoLDER NDVI data by neural network analysis (Weiss et al. 2002) and the land cover type map was retrieved from SPOT satellite scenes and field observations through a supervised classification analysis (Oliosio et al. 2002b).

### 4.2 The meteorological data

The upper boundary atmospheric conditions are from local radiosoundings for three days and from the Arpège meteorological model for 18 days. The Arpège meteorological model results from Météo France may not represent the local area of the Alpilles very well due to the coarse horizontal grid resolution of around 30 km. However comparison of the Arpège grid air temperatures to the local radiosounding observations shows a good correspondance. The Arpège air temperatures are slightly higher than the radiosounding observations in all cases. This is reassuring as the radiosoundings are probed higher (53, 42 and 46 m) in the atmosphere than the Arpège grid level.

The local air temperatures at the 2 m level measured in a well-watered alfalfa field are also compared successfully to the Arpège temperatures (Fig. 5). In this well-watered alfalfa field *H* is low and the atmospheric condition – very locally – has near-neutral stability. Therefore it is to be expected that the 2m air temperature will be quite similar to the temperature aloft.

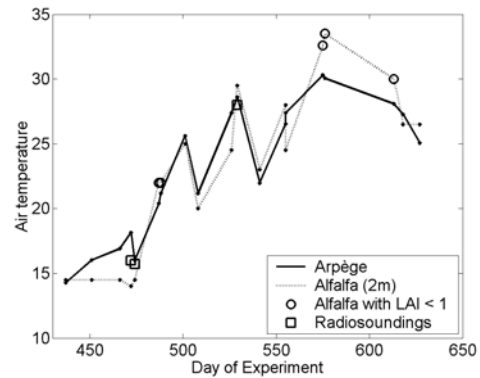


Figure 5 The Arpège meteorological air temperatures at 25 m and the surface air temperature at 2 m in a well-watered alfalfa field at the Alpilles site.

Furthermore the Arpège air temperatures are compared to the average and minimum surface temperatures in the airborne surface temperature maps. As all cases were acquired around noon in the growing season in the southern part of France, the average land surface temperature was always hotter than the average air temperature aloft (unstable conditions). The minimum surface temperature was determined from the *NDVI-Ts* minimum method.

The minimum surface temperature was on average around 10 °C cooler than the average surface temperature in the thermal maps. The minimum surface temperature in the maps was most often found in forest but sometimes in well-watered crops. In the case of near-neutral static stability the air temperature aloft would be close to the minimum surface temperature. The Arpège air temperature is lower (-1.6 °C) than the minimum surface temperature in only one case and within 2 °C in 11 cases out of 23 cases. This indicates that there typically is not local inversions (as expected) and that the minimum surface temperature may be found aloft at a (much) higher level in the atmosphere.

The wind speeds from the Arpège meteorological model, local field observations and radiosoundings in the Alpilles area are successfully compared in figure 6 at the times of thermal image data acquisition. The difference in wind speed between the Arpège data and field observations are on average 0.7 m s<sup>-1</sup> with a maximum of 3 m s<sup>-1</sup> and a standard deviation of 1.45 m s<sup>-1</sup>.

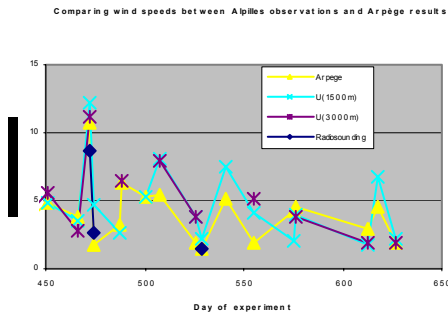


Figure 6 Comparing wind speeds from the Arpège meteorological model at 25 m grid level, field observations at 2m and radiosounding observations at 53, 42 and 46m in the Alpilles area at the times of thermal image data acquisition of 1500 m and 3000m flight levels.

#### 4.3 Microscale aggregation model results

Previously the microscale aggregation model has been run with a fixed ratio between the effective roughness lengths of 0.1, 0.01 and 0.001 on the Alpilles data set. It was found that a ratio of 0.01 ( $kB^{-1}$  of 4.6) gave the best correspondence between field based  $H$  observations and aggregation model results (Hasager et al. 2002b). The bias was near zero and the rmse around  $80 \text{ W m}^{-2}$ . The model results on  $H$  were better with input of radiosounding data indicating that these locally are more precise than the Arpège data.

The new aggregation model results on  $kB^{-1}$  is shown in figure 7. The directly calculated values of  $kB^{-1}$  range from 5 to 9, i.e. they are somewhat larger than previously found ( $kB^{-1}$  4.6).

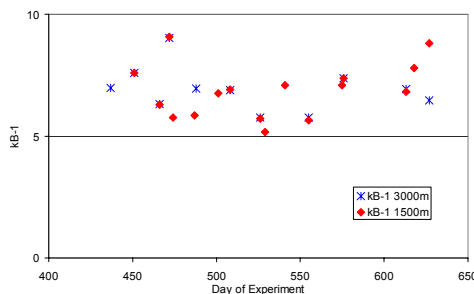


Figure 7 The  $kB^{-1}$  values calculated directly by the aggregation model for the cases in the Alpilles site.

The comparison between in-situ ground measurements of  $H$  and the new model results are graphed in figure 8a and b for input of radiosounding data and Arpège data, respectively. It is seen that there is a bias around  $30 \text{ W m}^{-2}$  for both but that the rmse is lower for input of radiosounding (around  $70 \text{ W m}^{-2}$ ) than for Arpège data (around  $85 \text{ W m}^{-2}$ ). This means that there is not obtained any significant improvement on the calculation of  $H$  compared to the results in Hasager et al. (2002b). It is however a great advantage that the ratio between the roughness for momentum and scalar fluxes did not have to be guessed.

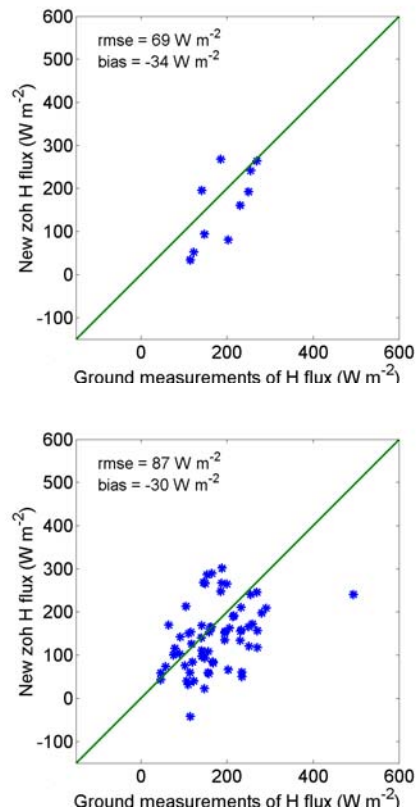


Figure 8 a) Comparison of in-situ ground observations of sensible heat ( $H$ ) flux to the new aggregation model results for local radiosounding input, b) for Arpège data.

The new  $H$  results are compared to the previous  $H$  model results (Hasager et al. 2002b) for all data points corresponding in space to ground flux observations and the comparison is shown in figure 9. It seems that two sets of observations each belonging to a different linear regression line exists. The results are preliminary as no in-depth study has been carried out yet to explain this result.

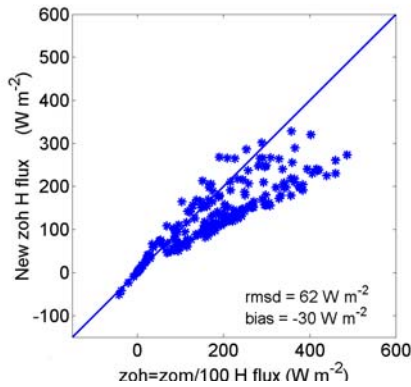


Figure 9 Comparison of sensible heat flux ( $H$ ) from assuming  $kB^{-1}$  4.6 and the new  $H$  result with direct calculation of  $kB^{-1}$  for all data points corresponding in space to ground flux observations.

For non-vegetated surfaces there is a constant ratio between the local values of  $z_0$  and  $z_{0t}$  but for vegetated surfaces the ratio is dependent upon vegetation type and  $LAI$ . Therefore  $\langle z_0 \rangle$  and  $\langle z_{0t} \rangle$  are no longer proportional in (partly) vegetated terrain. This effect is demonstrated for the Alpilles area for day of experiment 487 where the mean  $LAI$  was 1.123. It is now (artificially) assumed that the whole area possess this value of  $LAI$  as well as mean values ranging from 0.5 to 6.0  $LAI$ . The effective  $\langle z_{0t} \rangle$  values are graphed as a function of  $LAI$  in figure 10.

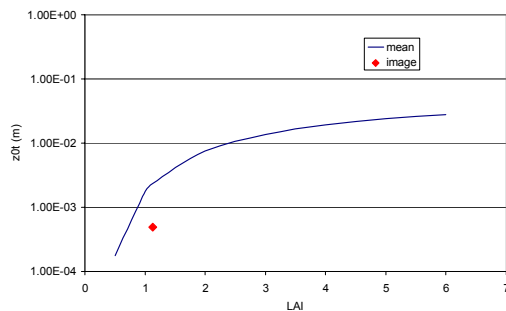


Figure 10 The  $\langle z_{0t} \rangle$  value calculated directly by the aggregation model for mean  $LAI$  values assumed to range from 0.5 to 6.0 at the Alpilles site. The result for the actual spatial variation is also shown ('image').

It is found that  $\langle z_{0t} \rangle$  including the actual (real) spatial variations in  $LAI$  is lower than assuming a mean  $LAI$  value. For large values of  $LAI$ ,  $\langle z_{0t} \rangle$  levels off to a nearly constant value whereas for decreasing values of  $LAI$   $\langle z_{0t} \rangle$  rapidly decreases. This indicates that  $\langle z_{0t} \rangle$

is very variable in areas of relatively low  $LAI$  values. Furthermore it demonstrates that the spatial variations of  $LAI$  are of great importance.

## 5 CONCLUSION

A new version of the physically-based surface-flux microscale aggregation model (original model described in Hasager and Jensen, 1999) is presented theoretically and applied on the Alpilles data set. The new development include the additional input of land cover type and  $LAI$  maps to the model in order to calculate not only the effective roughness for momentum  $\langle z_0 \rangle$  but also the effective roughness for scalars  $\langle z_{0t} \rangle$  directly. It is shown that the logarithmic ratio between  $\langle z_0 \rangle$  and  $\langle z_{0t} \rangle$  ranges from 5 to 9 for the 18 days studied at the Alpilles site based on airborne thermal images,  $LAI$  maps from airborne PoLDER NDVI, land cover maps from SPOT and air temperatures, wind speed and wind direction from local radiosoundings and Arpège data. A value of  $kB^{-1}$  2.3 is often assumed valid (in homogeneous terrain) but experimental data (from heterogeneous sites) have shown much larger values (e.g. up to 25). The new directly calculated values confirms the general experimental evidence that  $kB^{-1}$  is much larger than 2.3 in heterogeneous terrain.

Comparison of in-situ surface sensible heat flux from ground observations in various crops in the Alpilles area to the new aggregation model results shows a bias around 30  $W m^{-2}$  and rmse around 70  $W m^{-2}$  for radiosounding observation input and rmse around 85  $W m^{-2}$  for Arpège data input. This is not significantly better than if assuming  $kB^{-1}$  4.6 but the great advantage is that no assumption has to be taken. The results for the Alpilles site are preliminary as further investigation is on-going.

## 6 OUTLOOK

After ascertaining that the local  $H$  flux estimates are in accordance with in-situ observations, it is possible to area-average the flux at the 1 km grid scale comparable to NOAA AVHRR resolution. Sensible heat flux estimated from the microscale aggregation model at the larger scale may then be used as a guideline for the applicability of certain simpler surface-flux calculation methods at that scale.

## Acknowledgements

The EC 5<sup>th</sup> framework WATERMED project funding ICA3-CT-1999-00015 for application of the aggregation model to the Alpilles data set and the SAT-MAP-CLIMATE project funding from the

Danish Research Agency, Space Research Grant 5006-00-0063, for development of the new model version is gratefully acknowledged.

## REFERENCES

- Charnock, H. 1955 Wind stress on a water surface. *Quart. J. Royal Met. Soc.*, 81, 639-640
- Garratt J.R. and B.B. Hicks (1973) Momentum heat and water vapour transfer to and from natural and artificial surfaces. *Q.J.R.Met.Soc.*, **99**, 680-687.
- Hasager C.B. 1997. Surface fluxes in heterogeneous landscape. *Ph.D. dissertation. Risø-R-922(EN)*, 177p
- Hasager, C.B. & Jensen, N.O. 1999 Surface-flux aggregation in heterogeneous terrain, *Quart. J. Roy. Met. Soc.* **125**, 2075-2102.
- Hasager, C.B., Nielsen, N.W., Jensen, N.O., Christensen, J.H., Dellwik, E., Soegaard, H., and Boegh, E. 2002 Effective roughness calculated from satellite-derived land cover maps and hedge information and used in a weather forecasting model. *Boundary-Layer Meteorology* (submitted).
- Hasager, C.B.; Olioso, A.; Jacob, F., 2002b Parametrisation of aggregated roughness and sensible heat flux from field scale to hydrological scale by microscale modelling in the Alpilles experiment in France. EGS 2002, 27. General assembly, Nice (FR), 21-26 Apr 2002. *Geophys. Res. Abstr. (CD-ROM)* (2002) 4. See [abstract](#) and [poster](#)
- Jacob, F., Olioso, A., Gu, X.F., Su, Z., and Seguin, B., 2002, Mapping surface fluxes using airborne visible, near infrared, thermal infrared remote sensing data and a spatialized surface energy balance model. *Agronomie*, 22, in press.
- Jensen, N.O., Hasager, C.B. and Larsen, S.E. 2002 Aggregation of momentum and temperature roughnesses based on satellite data. European Geophysical Society 2002, XXVII General Assembly, Nice, France, 21-26 April, *Geophys. Research Abstracts*. (CD-ROM) See [abstract](#)
- Jensen N.O. and P. Hummelshøj (1995) Derivation of canopy resistance for water vapour fluxes over a spruce forest, using a new technique for the viscous sublayer resistance. *Agri. and Forest Met.*, **73**, 339-352.
- Jensen N.O. and P. Hummelshøj (1997) Erratum to "Derivation of canopy resistance for water vapour fluxes over a spruce forest, using a new technique for the viscous sublayer resistance". *Agri. and Forest Met.*, **85**, 289.
- Mölder, M., Sugita, M., Hiyama, T., and Bergstrom, H.: 1998, 'Regional Sensible Heat Flux and Thermal Roughness Length of an Inhomogeneous Landscape', *Hydrological Processes* 2115-2131
- Olioso, A., Braud, I., Chanzy, A., Demarty, J., Ducros, Y., Gaudu, J.-C., Gonzalez-Sosa, E., Lewan, E., Marloie, O., Ottlé, C., Prévot, L., Thony, J.-L., Autret, H., Bethenod, O., Bonnefond, J.-M., Bruguier, N., Buis, J.-P., Calvet, J.-C., Caselles, V., Chauki, H., Coll, C., François, C., Goujet, R., Jongschaap, R., Kerr, Y., King, C., Lagouarde, J.-P., Laurent, J.-P., Lecharpentier, P., Mc Aneney, J., Moulin, S., Rubio, E., Weiss, M., and Wigneron, J.-P., 2002, Monitoring energy and mass transfers during the Alpilles-ReSeDA experiment. *Agronomie*, 22, in press.
- Olioso, A., Hasager, C., Jacob, F., Wassenaar, T., Chehbouni, A., and Marloie, O., 2002, Mapping surface sensible heat fluxes from thermal infrared and reflectances data using various models over the Alpilles test site. First International Symposium on Recent Advances in Quantitative Remote Sensing, 16-20 September 2002, Valencia, Spain.
- Sellers P.J., D.A.Randall, G.J.Collatz, J.A.Berry, C.B.Field, D.A.Dazlich, C.Zhang, G.D.Collelo and L.Bounoua, 1996, A revised land surface parameterization (SiB2) for atmospheric GCMs. Part I. Model formulation., *J.Climate* Vol 9, no 4, p676-705
- Viterbo, P., 1996, The representation of surface processes in general circulation models, European Centre for Medium-Range Weather Forecasts, Reading, UK, pp201
- Wassenaar, T., Olioso, A., Hasager, C., Jacobs, F., Chehbouni, A. 2002 Estimation of evapotranspiration on heterogeneous pixels. In: *Proceedings of 1<sup>st</sup> international conference on Recent Advances in Quantitative Remote Sensing* (this issue)
- Weiss, M., Baret, F., Leroy, M., Hauteçæer, O., Bacour, C., Prévot, L., Bruguier, N. 2002 Validation of neural net techniques to estimate canopy biophysical variables from remote sensing. *Agronomie* 22
- Wood N. and P.Mason, 1991. The influence of static stability on the effective roughness lengths for momentum and heat transfer, *Q.J.R.Meteorol.Soc.* 117, 1025-1056